METEOROLOGICAL APPLICATIONS
Meteorol. Appl. **21**: 50–61 (2014)
Published online 27 February 2012 in Wiley Online Library
(wileyonlinelibrary.com) DOI: 10.1002/met.1296

A case study of missed approach of aircraft due to tailwind associated with thunderstorms

S. M. Tse, P. W. Chan* and W. K. Wong
Hong Kong Observatory, Hong Kong, China

ABSTRACT: Two aircraft had to conduct missed approaches in the overnight period of 8–9 September 2010 due to intense thunderstorm activity at the Hong Kong International Airport (HKIA). The missed approach event is studied in detail in this paper using the available flight data and other meteorological measurements. It appeared that the missed approaches were attributable to strong tailwind associated with the downdraft of the thunderstorm. Timely wind shear/microburst alerts had been provided to the pilots in this case based on the measurements from a Terminal Doppler Weather Radar (TDWR) and ground-based anemometer measurements at HKIA. The nowcasting and forecasting aspects for such an event are also discussed. The Aviation Thunderstorm Nowcasting System (ATNS) developed by the Hong Kong Observatory (HKO) is found to provide adequate nowcasting of thunderstorm activity for this particular case and the aviation weather forecasters could be alerted of such intense convective weather at the airport more than half an hour ahead. On the forecasting side, the mesoscale meteorological model used by HKO may provide an indication of the strong tailwind associated with the thunderstorm at 6–7 h ahead, though the exact timing of the tailwind at the airport may be delayed by a couple of hours compared with the actual situation. Using the model the downdraft of the thunderstorm in this event is examined in detail.

KEY WORDS missed approach; thunderstorm; windshear; nowcasting; fine-scale NWP

Received 14 August 2011; Revised 10 November 2011; Accepted 22 December 2011

1. Introduction

Hong Kong is situated in a subtropical region on the south-eastern coast of mainland China. In summer, the southwest monsoon and tropical cyclones are two typical types of weather conditions which are convective in nature. The convective weather not only brings showers and thunderstorms to the region, but disrupts air traffic.

Inclement weather may lead to significant disturbance to airport operation. For example, significant terrain-induced wind shear events in Hong Kong International Airport (HKIA) resulted in diversion of three aircraft on 27 December 2009 (Chan, 2011a) and a tail strike event on 5 March 2010 (Chan, 2011b). A tornado outbreak in Barcelona on 7 September 2005 caused extensive damage at the Barcelona International Airport and the airport was closed for 1 h (Bech *et al*., 2007).

HKIA is one of the busiest airports in the world. In 2010, HKIA handled more than 300 000 flight movements, with more than 800 flight movements a day on average. There were 39 aircraft diversions in that year, i.e. around 0.01% of the total flight movements, due to adverse weather including significant wind shear, turbulence and convective weather, according to the information from Civil Aviation Department of Hong Kong Special Administrator Region. Seventeen out of the 39 diversions took place in the overnight period of 8–9 September 2010 because of intense thunderstorm activity. From the available air traffic control information, two aircraft had to conduct missed approaches.

* Correspondence to: P. W. Chan, Hong Kong Observatory, 134A Nathan Road, Kowloon, Hong Kong, China.
E-mail: pwchan@hko.gov.hk

The missed approaches and subsequent diversion events were analysed in this paper using flight data and meteorological information. Observations from various meteorological equipment inside and around HKIA were used to reveal the meteorological conditions during the missed approaches. Nowcasting and forecasting aspects for the event are also discussed.

2. Synopsis of the event

The missed approaches at HKIA took place during the overnight period of 8–9 September 2010 when intense thunderstorm activity brought heavy rain and frequent lightning to the whole of Hong Kong. During this period, an intense rain band with north-south orientation swept from east to west across Hong Kong. More than 50 mm of rainfall in an hour were generally recorded over the territory and 13 102 cloud-to-ground lightning strokes were registered over the land and sea areas of Hong Kong (around 2700 km^2) during the hour just after midnight. The lightning number was the record-breaking number in an hour since records of lightning data of Hong Kong Observatory began in 2005. When the thunderstorms moved close to HKIA which was situated at the western part of the territory, gusty strong easterlies from the downdraft of the thunderstorm first affected the flight paths east of the airport resulting in an abrupt change in the prevailing winds from southwesterlies to easterlies.

Two flights which tried to land as the thunderstorms approached HKIA aborted landing and diverted to Macao (about 40 km southwest of HKIA). Both flights approached HKIA from the east under the prevailing southwesterly winds (Figure 1). Wind shear and microburst alerts were relayed to

Figure 1. Flight paths of the two aircraft which had to conduct missed approach. Red line indicates the flight path for the first aircraft and blue for the second aircraft. Black wind barbs showed the locations of aircraft when tailwind was encountered. The first and second aircraft recorded tailwind of 37 and 22 knots (68.5 and 40.7 km h^{-1}) respectively.

pilots *via* air traffic controllers. The first aircraft went around twice. The first aborted landing was due to technical consideration. In the second approach at around 0008 Hong Kong Time (HKT: HKT = UTC + 8 h) it encountered a strong tailwind. Landing was subsequently aborted and the aircraft diverted. Four minutes later, the second aircraft followed the same glide path as the first and also aborted the landing due to the strong tailwind. The aircraft was also diverted to Macao at 0012 HKT.

3. Analysis of aircraft data

Flight data retrieved from the flight data recorders of the two aircraft were analysed to reveal the meteorological conditions encountered by the aircraft. It appeared that the missed approaches were attributable to the strong tailwind which exceeded the airline's pre-defined threshold, of 15 knots (27.8 km h^{-1}) measured by anemometers for tailwind landing.

According to the flight data, the first aircraft experienced more than 15 knots of tailwind after it descended to below 1600 feet (488 m; Figure 2(a)) in its second approach. The tailwind increased from 25 knots (46.3 km h^{-1}) when the aircraft descended to 780 feet (238 m; 'A' in Figure 2(a)) to 37 knots (68.5 km h^{-1}) at 708 feet (216 m) at 0008 HKT ('B' in Figure 2). As a result, the diversion to another airport was conducted.

The second aircraft also experienced a tailwind of around 15 knots when it descended to around 1600 feet (488 m). The tailwind increased and reached 19 knots (35.2 km h^{-1}) when the aircraft descended to 1423 feet (434 m; 'C' in Figure 2(b)) but then decreased and fluctuated between 7 and 12 knots (13.0 to 22.2 km h^{-1}) when the aircraft further descended to 1028 feet (313 m; 'D' in Figure 2(b)). At around 0012 HKT, the tailwind started to strengthen again and exceeded 15 knots. The maximum tailwind experienced by the aircraft was 22 knots (40.7 km h^{-1}) at 859 feet (262 m) above the runway ('E' in Figure 2(b)). Similar to the first aircraft, the second aircraft executed a missed approach due to the strong tailwind and was diverted.

4. Synoptic and mesoscale weather conditions

In order to understand the development of the intense thunderstorm affecting the air traffic, synoptic and mesoscale weather conditions were studied. On 8 September 2010, Tropical Depression Meranti was situated to the southwest of Taiwan (Figure 3) and moved generally westwards. The southeastern coast of China had a clear sky and weak surface pressure gradient. Over Hong Kong, surface winds were light. North to northeasterly winds prevailed aloft (not shown) according to the Hong Kong tephigram at 2000 HKT. Meanwhile, an upper-cold low was centred to the east of Taiwan. The divergence area at 200 hPa to the west of the upper cold low affected the southeastern coast of China, which could enhance convective development.

Temperatures over most parts of Guangdong, China rose to 34 °C or above in the afternoon under abundant sunshine. Temperatures of some places inland even reached 37 °C. The weak surface northerlies brought a hot continental airstream to Hong Kong. The temperature at Hong Kong rose to 34 °C in the afternoon. The K-index and Convective Available Potential Energy (CAPE) at Hong Kong were as high as 41 °C and above 5000 J kg^{-1} respectively at 2000 HKT, implying that the atmosphere was very unstable (National Weather Service Weather Forecast Office, 2011).

Detailed analysis of surface winds revealed a convergence zone around 220 km northeast of HKIA, around 23°N 116 °E, for which radar echoes associated with heat showers started to emerge at 1530 HKT, as illustrated from the Hong Kong

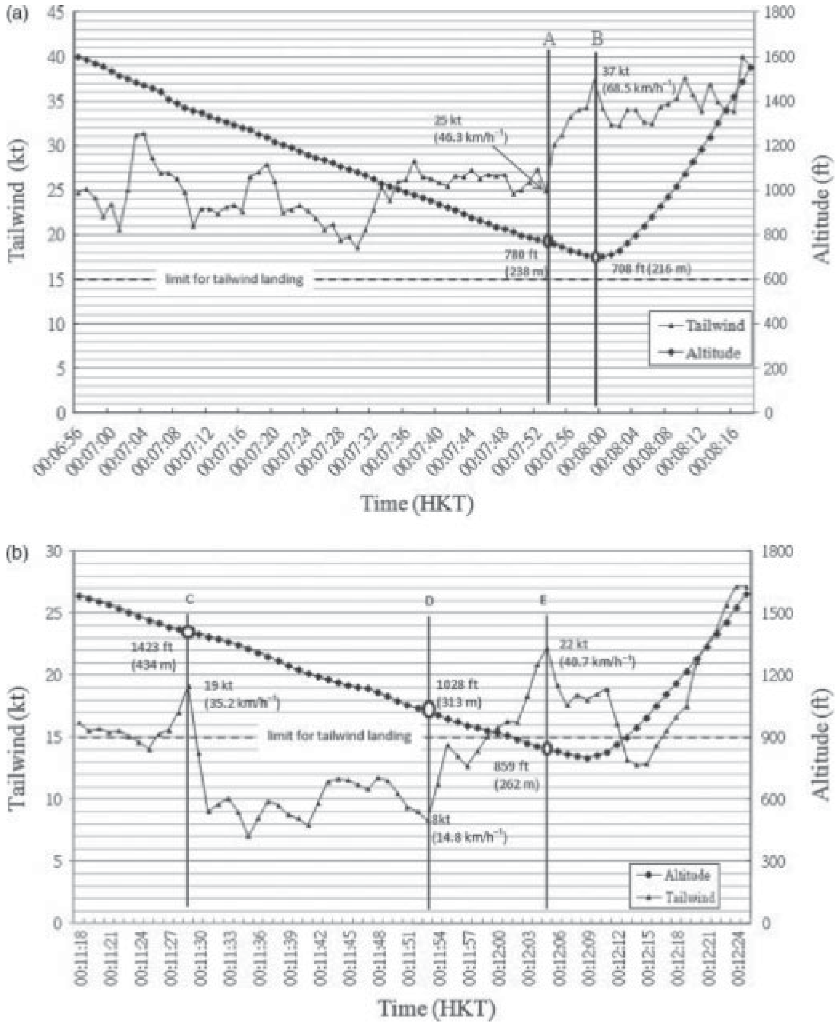

Figure 2. Time series in HKT of tailwind in knots (triangle) and aircraft altitude in feet (diamond) retrieved from the flight data recorders. (a) Flight data for the first aircraft. Tailwind reached 37 knots (68.5 km h^{-1}) at 0008 HKT. (b) Flight data for the second aircraft.

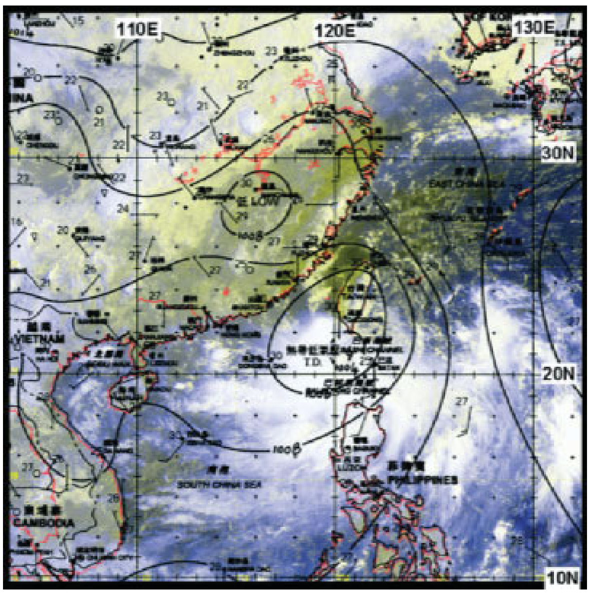

Figure 3. A false-colour satellite image at 0008 HKT on 8 September 2010 overlaid by a surface chart. Tropical Depression Meranti (T.D.) was at the southwest of Taiwan. The location of Hong Kong is marked by a red star.

Observatory (HKO) weather radar images. The heat showers developed over the convergence zone drifted southwestwards with a convective cell extended southwards. Convection continued to be sustained in the evening even though the echoes moved to cooler sea surface (Figure 4). Furthermore, echoes evolved into two organized bands at 2200 HKT; an intense band was 20 km east of HKIA and a weaker band was around 100 km. The development of the intense band was associated with a confluence zone which was clearly illustrated by the streamline analysis based on Hong Kong and Guangdong automatic weather station data (Figure 5) at 2000 HKT. The leading edge of the rain band started to affect HKIA at around 2318 HKT. The intense part of the rain band moved across HKIA from 2318 HKT to around 0100 HKT and brought heavy rain and frequent lightning to HKIA. The aviation forecaster at HKIA issued the aerodrome thunderstorm warning at around 2230 HKT on 8 September to alert pilots in advance about the significant convective weather.

5. Meteorological observations near the airport

HKO operates a network of meteorological equipment, including wind profilers, surface anemometers, Terminal Doppler Weather Radar (TDWR) and LIDAR systems inside and around

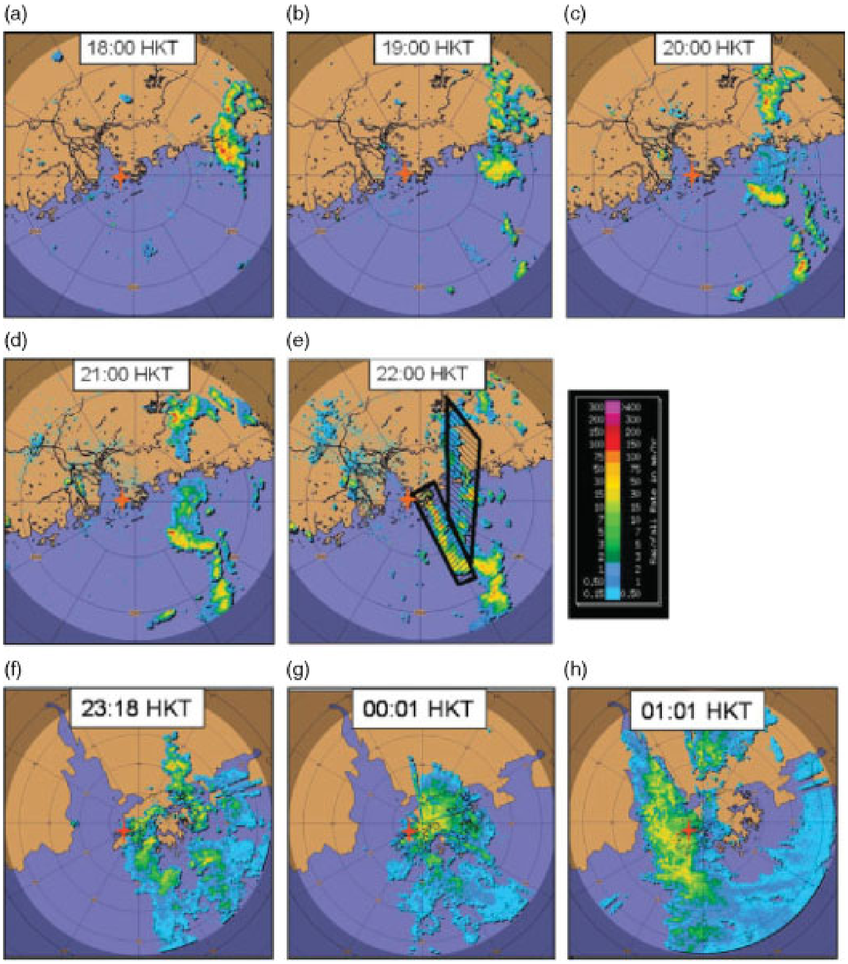

Figure 4. A series of radar images showing the development of echoes from 1800 HKT of 8 September 2010 to 0101 HKT of 8 September 2010. Bands of echoes drifted southwestwards towards HKIA (orange star) with convective cell extended southwards and remained strong over the sea. Two bands of echoes appeared at 2200 HKT (hatched regions). Intense echoes started to affect HKIA around 2318 HKT Parts (a) to (e) are CAPPI images at 3 km from HKO weather radar. Range rings at 50 km intervals. Parts (f) to (h) are PPI images from TDWR with antenna angle at 0.6°. Range rings at 20 km intervals.

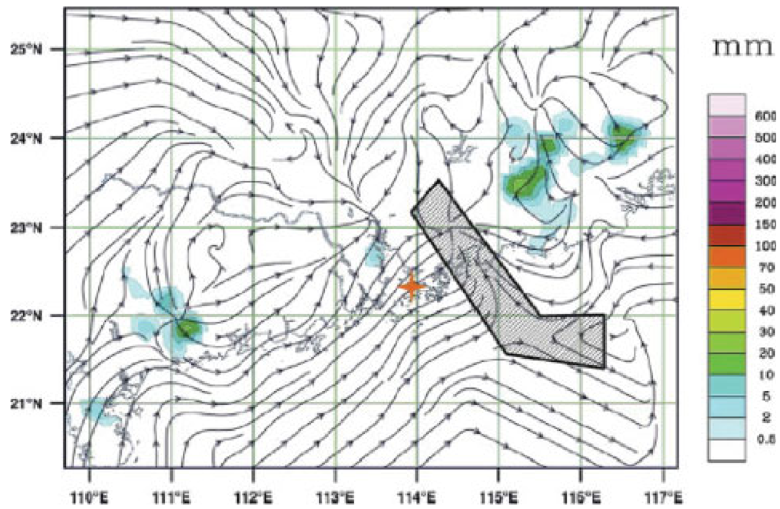

Figure 5. Streamline analysis (thick black line) and 1-hour precipitation (shaded area, in millimetres) based on Hong Kong and Guangdong automatic weather station data at 2000 HKT of 8 September 2010. Surface wind data are 10 min average at corresponding station levels. The Cressman method is used to construct grid-point winds based on AWS data only. A convergence zone (hatched area) was observed east of HKIA (orange star).

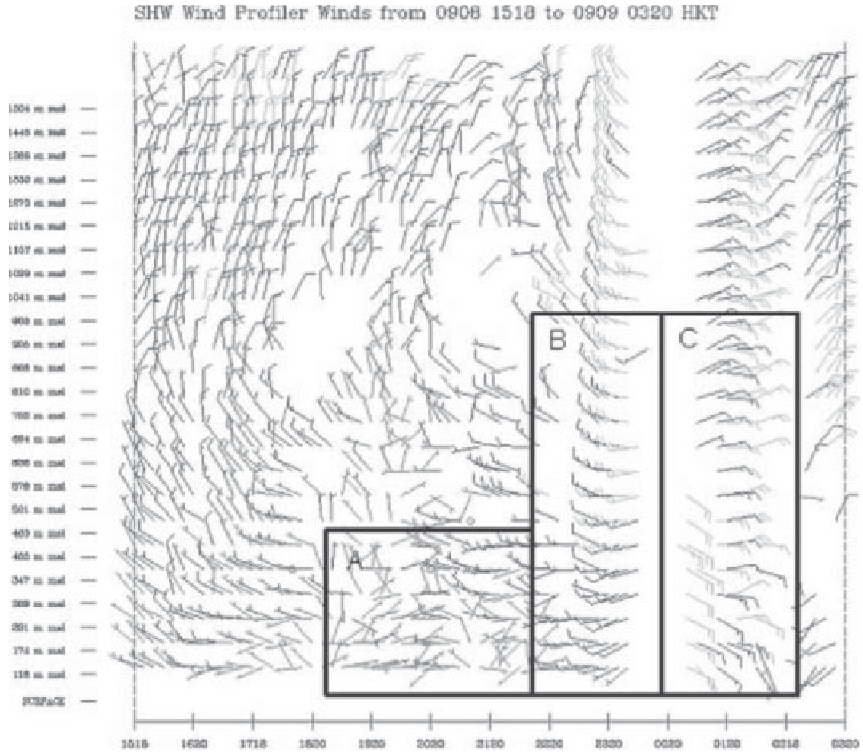

Figure 6. Wind profiles showing the changes of wind speed and directions in the evening of 8 September and in the small hours of 9 September 2010. (Area A) Weak winds; (Area B) winds strengthened from the west; (Area C) winds suddenly changed to easterlies.

HKIA to monitor the meteorological conditions closely. Except LIDAR, of which signals were highly attenuated due to precipitation, data obtained from these meteorological instruments were used to investigate the meteorological condition of the missed approach events.

Wind profiler data illustrated the evolution of the winds closed to HKIA as the convergence line associated with the thunderstorm moved across the station. Winds from the surface to 1000 m above ground remained weak in the evening (area A of Figure 6). Before midnight, winds strengthened from the west and became organized (area B) and then suddenly changed to easterlies after midnight (area C). The timing of the wind change agreed with the passage of the convergence line associated with the thunderstorm depicted in Figure 5.

Anemometers in and around HKIA also detected the change of the wind direction due to the thunderstorm (Figure 7). At 2354 HKT, the shear line, which was the leading edge of thunderstorm-induced easterlies, moved westwards and winds at two anemometers east of HKIA changed to easterlies. Easterlies measured by one of the two anemometers strengthened to more than 30 knots (55.6 km h^{-1}) 12 min later at 0006 HKT (around the time of the missed approach events), when the shear line moved to HKIA. Strong easterlies continued to extend westwards.

The TDWR also captured the wind conditions when the two aircraft conducted missed approaches. Figure 8(a) and (b) showed the radial velocity measured by TDWR at 0008 HKT and 0012 HKT 9 September respectively. Gusts reaching 27 m s^{-1} (around 50 knots) were captured by the TDWR over the eastern part of HKIA. The zero isotach, which marked the leading edge of the shear line, agreed well with that identified based on anemometer data.

The surface temperature at HKIA dropped sharply from 30 to 25 °C while the dew point dropped from 28 to 24 °C soon after midnight after the passage of the shear line indicating cooling due to the downdraft of the thunderstorm.

6. Alerts issued by the HKO Wind shear and Turbulence Alerting System

The HKO Wind shear and Turbulence Alerting System (WTWS) integrates wind shear and turbulence alerts generated by different algorithms such as the Anemometer-based Wind shear Alerting Rules-Enhanced (AWARE) (Lee, 2004), the LIDAR Wind shear Alerting System (LIWAS) (Shun and Chan, 2008), TDWR alerts and other algorithms. Alerts are then generated for eight runway corridors (the north runway and south runway have two arrival and two departure corridors each) and shown on a graphical display, the WTWS display.

At 0008 HKT, the zero isotach over HKIA detected by the TDWR was analysed as a gust front and was shown on the WTWS display (Figure 9(a)). In addition, microburst alerts, which represent wind shear loss of 30 knots (55.6 km h^{-1}) or more with precipitation, were provided by the TDWR to the east of HKIA: wind shear alerts were generated from AWARE over the runways; turbulence alerts were in force due to the thunderstorm. Over the eight corridors of HKIA, all had wind shear alerts with magnitude ranging from +25 to +30 knots (46.3–55.6 km h^{-1}). At 0012 HKT, although the gust front was not detected by the TDWR (Figure 9(b)) any more, using the surface anemometers and TDWR base data, wind shear alerts with magnitude ranging from +15 to +25 knots (27.8–46.3 km h^{-1}) were issued for the four western corridors. Meanwhile, areas with the microburst alerts shifted westwards and affected the eastern corridors. The WTWS issued microburst alerts of −35 knots (−64.8 km h^{-1})

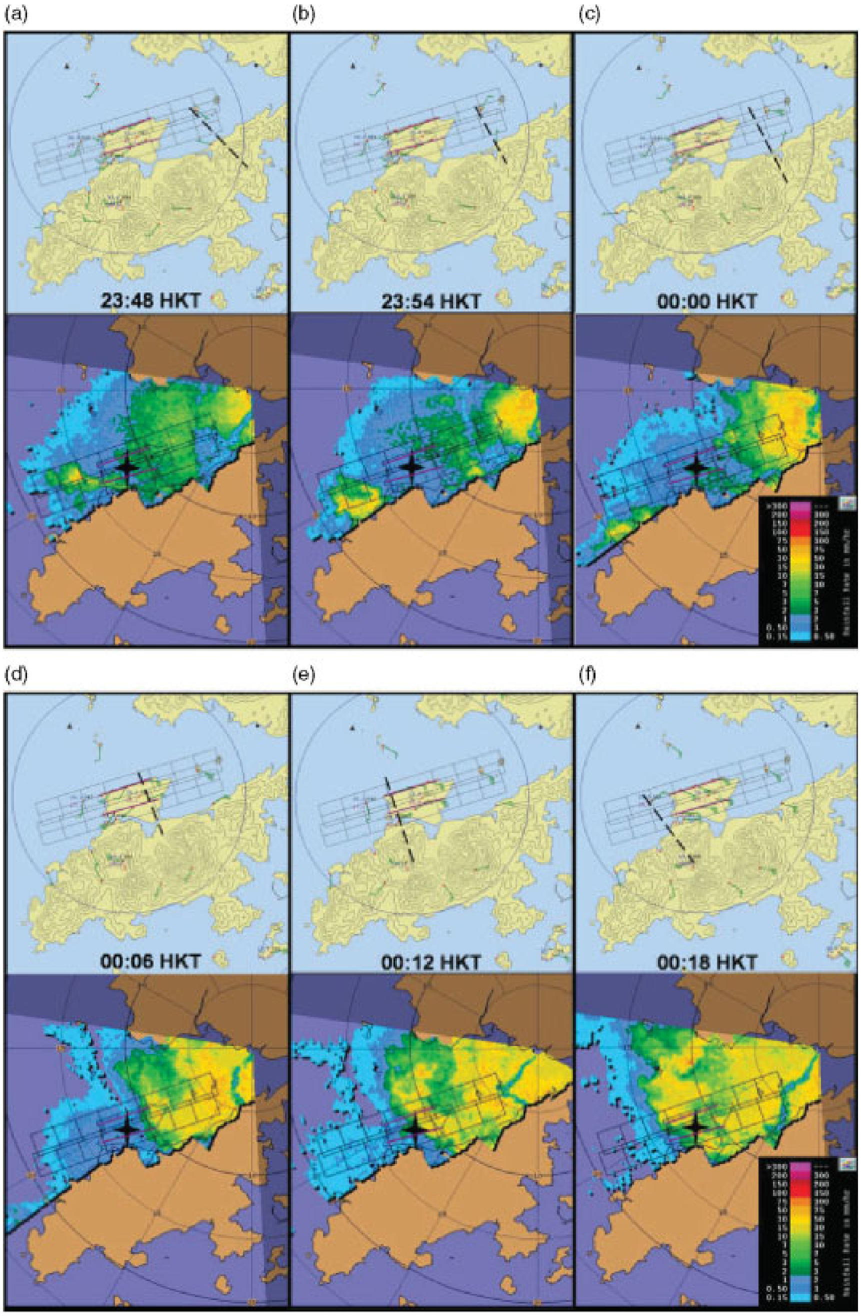

Figure 7. A sequence of pictures showing winds in the vicinity of HKIA (black star) and radar reflectivity nearby. Wind barbs (upper) showing the propagation of thunderstorm-related easterly wind and TDWR images (lower) showing the location of the rain band. Dashed line was the shear line or leading edge of easterlies which was near regions with the highest rainfall rate (75–100 mm h^{-1}, orange in radar images). Purple line marked two runways of HKIA.

to the four eastern corridors. During the event, the WTWS functioned properly and was able to provide adequate warning to the aircraft of the wind shear to be expected due to the thundery weather.

7. Nowcasting of thunderstorms

A nowcasting system named the Aviation Thunderstorm Nowcasting System (ATNS) was developed by HKO to provide forecast on the convective activities to support airline and air traffic management operations near HKIA (Li, 2009). It is a short-term prediction system that is based on weather radar data, and uses the Tracking Radar Echoes by Correlation (TREC) technique (Tuttle and Foote, 1990) and Semi-Lagrangian Advection Scheme to extrapolate thunderstorm motions for the next 60 min with an update frequency of every 6 min.

The ATNS was able to forecast the thunderstorm movement for the missed approach events. Figure 10(a) showed the ATNS forecast based on the last available weather radar images at 2236 HKT from one of the HKO weather radars which then malfunctioned in the following few hours due to frequent lightning. The ATNS forecast that the moderate to intense convective activities (band A of Figure 10(a)) to the east of HKIA would start to affect HKIA at 2312 HKT to the end

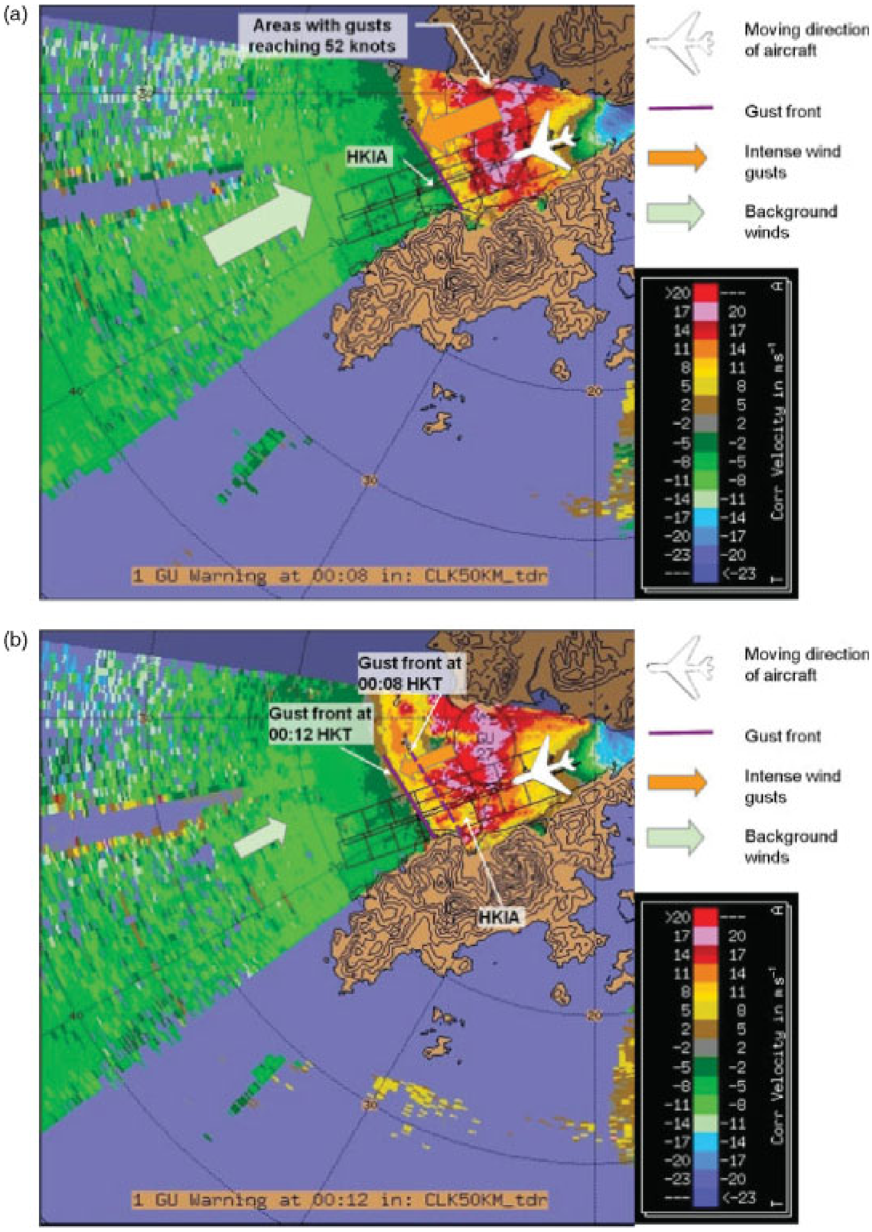

Figure 8. Velocity measured by TDWR on 9 September 2010. The cool/warm colours represented winds towards/away from the TDWR. PPI antenna angle was 0.6°. Range rings are at 10 km intervals. Area with gusts reaching 27 m s^{-1} are circled in black. The zero isotach (gust front) is in purple. Aircraft approached HKIA from the east. (a) TDWR image at 0008 HKT; (b) TDWR image at 0012 HKT. The zero isotach (gust front) moved westwards to the western end of HKIA.

of the forecasting period. The convective activity would be most intense during 2318–2330 HKT and regions with radar reflectivity more than 41 dBz would affect HKIA, which proved consistent with the actual situation as revealed by the TDWR image (Figure 10(b) and (c)). The lead time provided by the ATNS was more than half an hour. The system provided a useful tool to alert aviation forecasters in advance. However, the ATNS failed to forecast that another band of echoes (band B of Figure 10(a)) east of band A would start to affect HKIA around midnight as the ATNS used a constant speed to extrapolate the location of the rain bands throughout the forecast period. The actual situation was that ‘band B’ accelerated when moving west and merged with ‘band A’. Intense convective activity still affected HKIA at 2336 HKT (Figure 10(d)), which was under-estimated by the ATNS.

8. Forecasting of thunderstorms

Apart from a nowcasting system, the HKO also operates an NWP-based Rainstorm Analysis and Prediction Integrated Data-processing System- Non-Hydrostatic Model (RAPIDS-NHM) (Wong, 2010) to provide forecast for intense thunderstorms. The RAPIDS-NHM is part of the HKO mesoscale numerical weather prediction system called Atmospheric Integrated Rapid-cycle (AIR), which is based on the JMA NHM (Saito *et al*., 2006) and its three-dimensional variation data assimilation system (3DVAR). AIR consists of two domains: Meso-NHM is an outer domain with horizontal resolution of 10 km and 50 vertical levels and RAPIDS-NHM is an inner domain with horizontal resolution of 2 km and 60 vertical levels. The boundary conditions of RAPIDS-NHM are

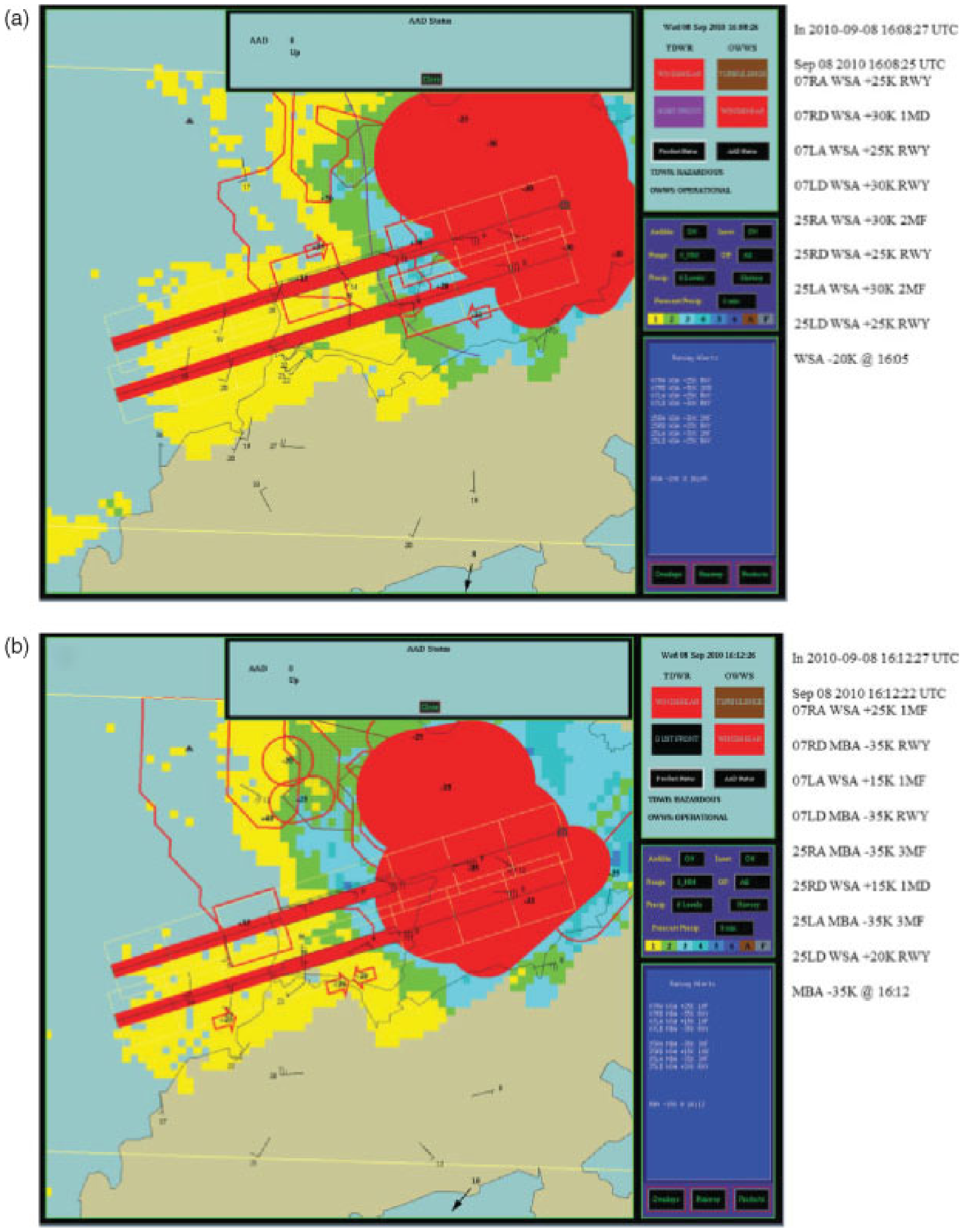

Figure 9. WTWS displays on 9 September 2010. Gust front analysed by TDWR (purple line) over HKIA; microburst alerts generated by TDWR (red solid band-aids); wind shear alerts generated by AWARE (red hollow rectangles), based on TDWR (red hollow irregular polygons); by LIDAR (red arrows, over the runways only); turbulence alert based on TDWR (brown polygon with dots). Black numbers were the wind shear magnitude in knots. (a) 0008 HKT on 9 September 2010. A gust front was over HKIA. Wind shear alerts were issued by the WTWS for all runway corridors. LIDAR data was highly attenuated by precipitation and could only detect wind shear over the runway. (b) 00 : 12 HKT on 9 September 2010. Microburst alerts of −35 knots (−64.8 km h^{-1}) were issued to the four eastern corridors. Wind shear alerts with magnitude ranging from +15 to +25 (+27.8 to +46.3 km h^{-1}) knots were issued for the four western corridors.

provided by Meso-NHM forecast in a one-way nesting configuration. RAPIDS-NHM provides forecast up to 15 h ahead and is executed every hour. The 3DVAR ingests observations including radar Doppler velocity, radar wind retrieval products, wind profilers, data from automatic weather stations from mesoscale observation networks in Hong Kong and the Guangdong Province and conventional observations from a synoptic station (Wong *et al*., 2011).

The model run at 1900 HKT (1100 UTC) of 8 September 2010 forecast a rain band, 'A', oriented north–south would be just to the east of HKIA 6 h later, i.e. 0100 HKT of 9 September 2010 (Figure 11). The model also forecast another less organized rain band, 'B', which was similar as the actual rain band pattern observed at 2200 HKT radar image (Figure 4(e)), although the locations of rain bands were slightly different and the forecast timing was 1–2 h later than the actual.

Figure 12 showed that there was a tight surface temperature gradient around 15 km to the east of HKIA forecast by RAPIDS-NHM. West of the tight temperature gradient region, surface temperature was high and westerlies prevailed. When the leading edge of the rain band moved past, surface temperature dropped and winds changed to easterlies. This was

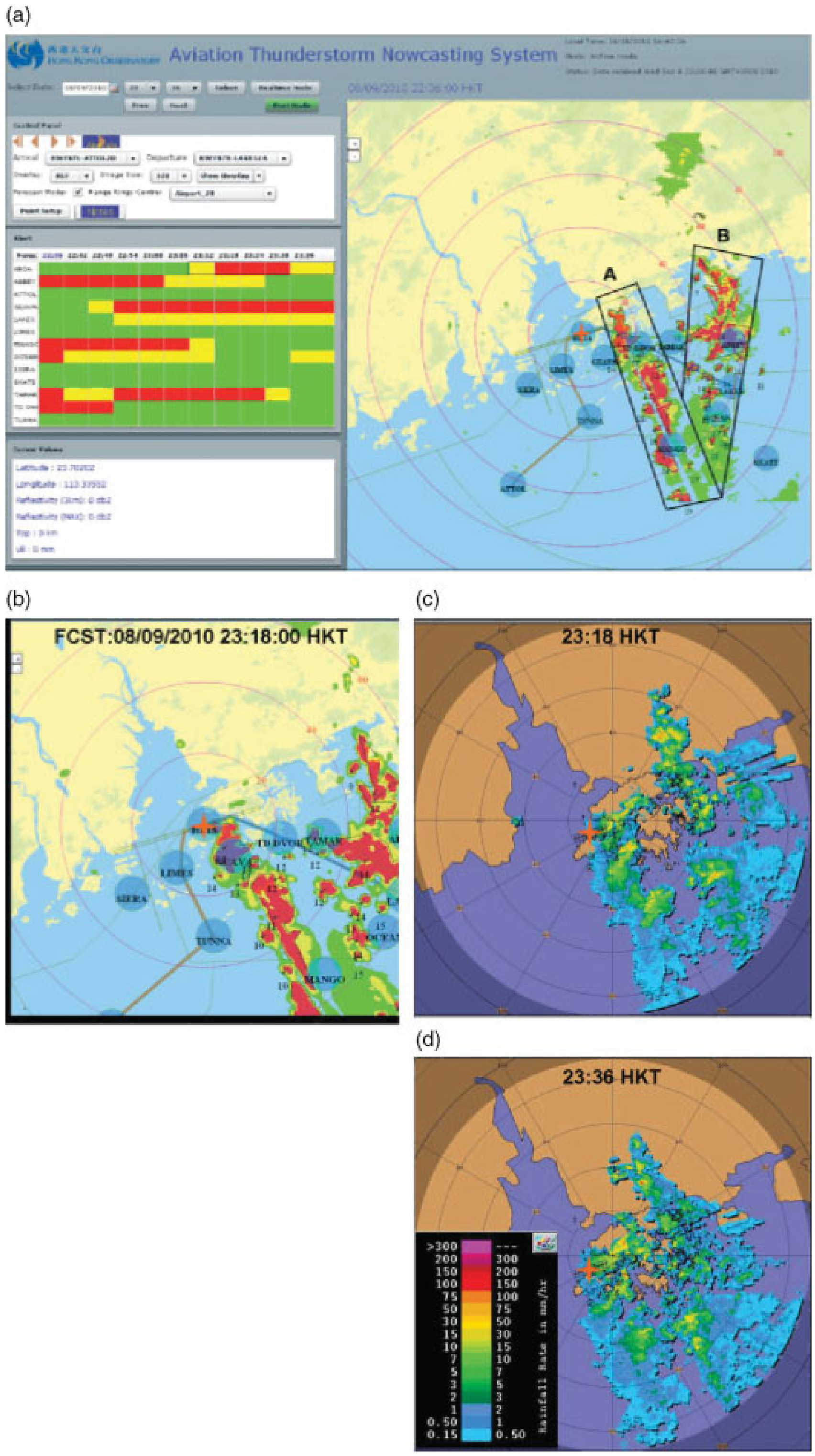

Figure 10. (a) ATNS display initiated at 2236 HKT. Range rings were at 10 nm (18.5 km) intervals. It forecast that moderate to intense convection activities would affect HKIA from 2312 HKT to the end of the forecasting period, i.e. 2336 HKT. Yellow and red on the left tabular panel indicated moderate (yellow, $\geq$33 dBz and <41 dBz) and intense (red, $\geq$41 dBz) activity activities. (b) ATNS forecast for 2318 HKT initiated at 2236 HKT. Range rings are at 10 nm (18.5 km) intervals. (c) TDWR image at 2318 HKT. Range rings are at 20 km intervals. (d) TDWR image at 2336 HKT. Range rings are at 20 km intervals. Location of HKIA is marked by an orange star.

consistent with what was actually observed. RAPIDS-NHM also forecast strong surface easterly winds (reaching 24 knots; 44.4 km h^{-1}) close to the leading edge of the cool air.

The forecast winds at 950 hPa (Figure 13(a)) an hour later, i.e. 0200 HKT of 9 September 2010, reached 37 knots (68.5 km h^{-1}) just to the east of HKIA (marked as 'X' on Figure 3(a)) which was where the aircraft encountered the strong tailwind. A vertical cross-section (Figure 13(b)) revealed the vertical structure of the thunderstorms with a strong equivalent potential temperature gradient ahead of the cool air (low

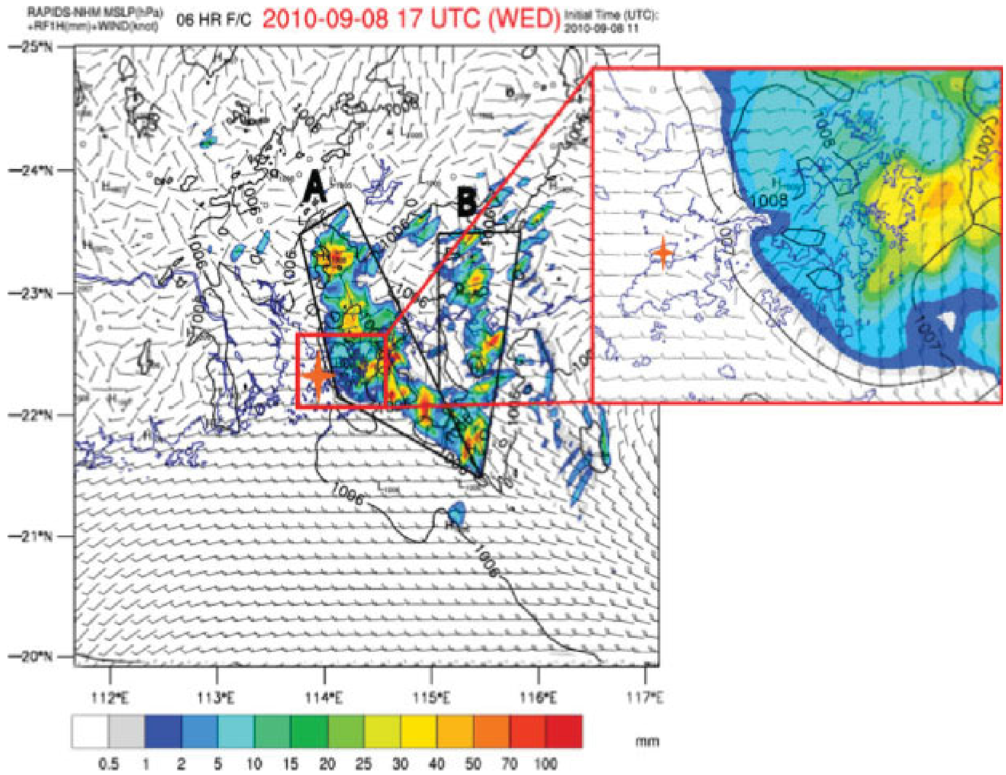

Figure 11. RAPIDS-NHM prognostic chart at the surface level showing winds (wind barb in knot), mean sea level pressure (black contour in hPa) and 1-h precipitation (shaded area in millimetres) at $T + 6$ h initiated at 19 HKT (1100 UTC) of 9 September 2010. The model forecast two rain bands would be just to the east of HKIA 6 h later. Location of HKIA is represented by an orange star. Enlarged image of the red box is on the right.

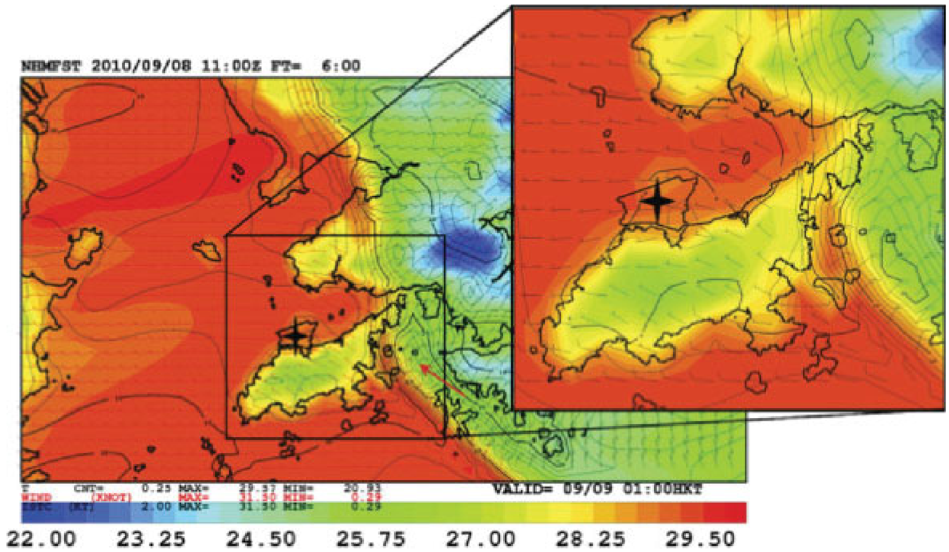

Figure 12. RAPIDS-NHM prognostic chart at the surface level showing winds (knots), isotach (black contour) and surface temperature (°C, shaded) at $T + 6$ h initiated at 1900 HKT (1100 UTC) of 9 September 2010. A region of surface winds reaching 24 knots (44.4 km h^{-1}) indicated by red arrow closed to the leading edge of the cool air was anticipated. Location of HKIA is marked by a black star. Enlarged image of the black box is on the right.

equivalent potential temperature). Warm air (high equivalent potential temperature) west of the strong gradient region was uplifted to 800 hPa. Cool air east of the strong gradient area descended to the surface and spread out close to the ground. This corroborated the observation that the strong tailwind encountered by two aircraft was associated with downdraft of the thunderstorm.

9. Conclusions

Two aircraft had to conduct missed approach to Hong Kong International Airport (HKIA) in the overnight period of 8–9 September 2010. A detailed study has been carried out to examine the meteorological situation during the missed approach events using flight data and meteorological

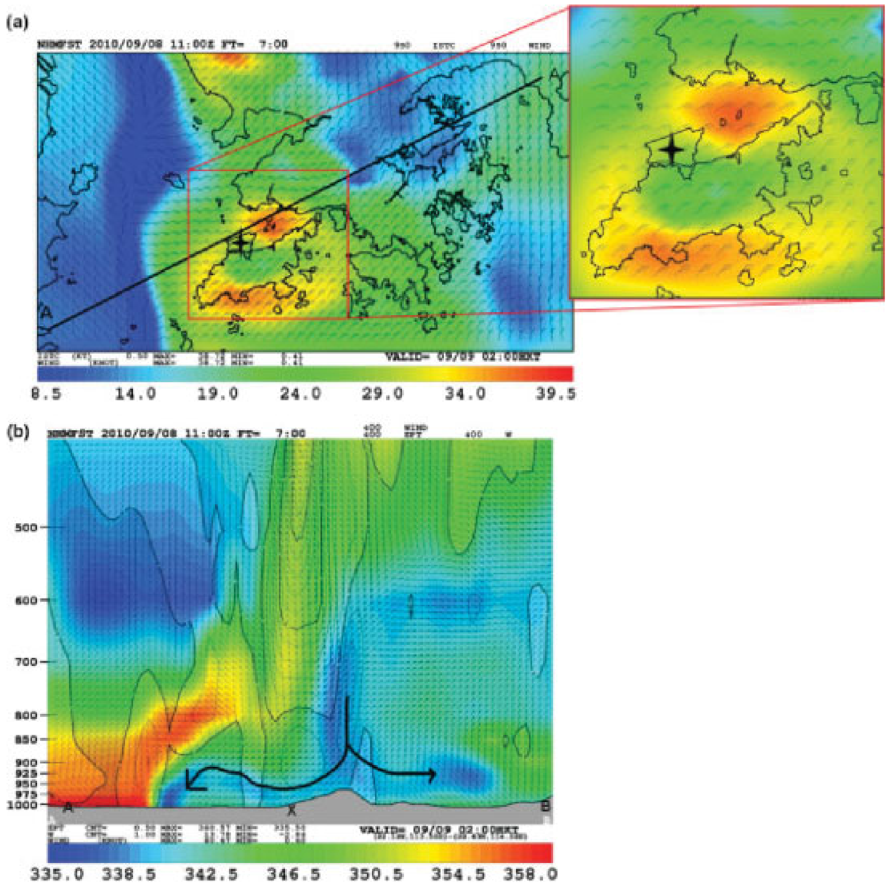

Figure 13. (a) RAPIDS-NHM prognostic chart at 950 hPa showing winds (knots, shaded at $T + 7$ h initiated at 1900 HKT (1100 UTC) of 9 September 2010. Location of HKIA is marked by a black star. A region of surface winds reaching 37 knots (68.5 km h^{-1}) at the northeast of HKIA (labeled as 'X') was anticipated. Enlarged image of the red box is on the right. (b) A vertical cross-section along A-B showing equivalent potential temperature (shaded area in Kelvin) and vertical velocity (black contour) and horizontal wind speed (wind barb). Regions with downward motions are hatched. Warm and moist air was uplifted while cool and dry air was brought to the surface and spread outwards near the surface.

measurements. Based on the available information, the missed approach events was attributed to strong tailwind associated with an intense thunderstorm.

The missed approach events were analysed based on the available meteorological observations. Prevailing southwesterly winds at HKIA changed to easterlies, strengthened and became gusty when the intense thunderstorms moved towards HKIA from the east. Gusts reaching 50 knots (92.6 km h^{-1}) as indicated by Terminal Doppler Weather Radar (TDWR) were found at or near the eastern corridors of HKIA when the two aircraft had to conduct missed approach. The sudden drop in surface temperature and dew point suggested that the strong tailwind was associated with the downdraft of the thunderstorm.

Timely wind shear and microburst alerts were issued by Wind shear and Turbulence Alerting System (WTWS). A gust front was identified by the TDWR over the airport. Meanwhile, a headwind change of more than 30 knots (55.6 km h^{-1}) was detected by TDWR and the Anemometer-based Wind shear Alerting Rules-Enhanced (AWARE) algorithm. The wind shear alerts were issued when the first aircraft approached HKIA at 0008 HKT of 9 September 2010. When the second aircraft approached HKIA 4 min later, microburst alerts were issued for the landing runway corridor.

The nowcasting and forecasting of the event were also studied. The Aviation Thunderstorm Nowcasting System (ATNS) was able to provide an early alert on the intense convective activity 30 min beforehand based on radar data, although the duration of the event was underestimated. The mesoscale model RAPIDS-NHM used by the HKO was capable to provide indication of the strong tailwind and gusts associated with the thunderstorm activity 6–7 h ahead, though the exact timing of the event was 2–3 h later than the actual situation. It successfully forecast gusts reaching 37 knots (68.5 km h^{-1}) around 950 hPa near HKIA and revealed the downdraft of the thunderstorm.

The capability of WTWS, ATNS and RAPIDS-NHM in alerting the aircraft for intense convective weather will be studied based on more cases in HKIA. In particular, the forecasting capability of ATNS and RAPIDS-NHM will be examined in more detail.

References

Bech J, Pascual R, Rigo T, Pineda N, López JM, Arús J, Gayà M. 2007. An observational study of the 7 September 2005 Barcelona tornado outbreak. *Nat. Hazards Earth Syst. Sci.* **7**: 129–139.

Chan PW. 2011a. A significant wind shear event leading to aircraft diversion at the Hong Kong International Airport. *Meteorol. Appl.* DOI: 10.1002/met.242.

Chan PW. 2011b. An event of tail strike of an aircraft due to terrain-induced wind shear at the Hong Kong International Airport. *Meteorol. Appl.* DOI: 10.1002/met.264.

Lee OSM. 2004. Enhancement of the anemometer-based system for wind shear detection at the Hong Kong International Airport. Presented in *Eighth Meeting of the Communications/Navigation/Surveillance and Meteorology Sub-Group (CNS/MET/SG/8) of APANPIRG, 12–16 July 2004, Bangkok*. International Civil Aviation Organization. http://www.hko.gov.hk/publica/reprint/r547.pdf

Li PW. 2009. Development of a thunderstorm nowcasting system in support of Air Traffic Management. *Aviation, Range, Aerospace Meteorology Special Symposium on Weather-Air Traffic Management Integration, 11–15 January 2009, Phoenix, AZ*. American Meteorological Society: Boston, MA. http://www.hko.gov.hk/publica/reprint/r873.pdf (accessed June 2011).

National Weather Service Weather Forecast Office. 2011. *Convective Season Environmental Parameters and Indices*. National Weather Service Weather Forecast Office: Louisville KY. http://www.crh.noaa.gov/lmk/soo/docu/indices.php (accessed October 2011).

Saito K, Fujita T, Yamada Y, Ishida J, Kumagai Y, Aranami K, Ohmori S, Nagasawa R, Kumagai S, Muroi C, Kato T, Eito H, Yamazaki Y. 2006. The operational JMA nonhydrostatic mesoscale model. *Mon. Weather Rev.* **134**: 1266–1298.

Shun CM, Chan PW. 2008. Applications of an infrared Doppler Lidar in detection of wind shear. *J. Atmos. Oceanic Technol.* **25**: 637–655. http://www.weather.gov.hk/publica/reprint/r776.pdf (accessed June 2011).

Tuttle JD, Foote GB. 1990. Determination of the boundary layer airflow from a single Doppler radar. *J. Atmos. Oceanic Technol.* **7**: 218–232.

Wong WK. 2010. Development of operational rapid update non-hydrostatic NWP and data assimilation systems in the Hong Kong Observatory. *The 3rd International Workshop on Prevention and Mitigation of Meteorological Disasters in Southeast Asia*, 1–4 March 2010, Beppu. http://www.hko.gov.hk/publica/reprint/r882.pdf (accessed June 2011).

Wong WK, Or MK, Chan PW, Cheng CM. 2011. Impact of radar retrieval winds on data assimilation and forecast of a mesoscale convective storm using Non-Hydrostatic Model. Presented in *14th Conference on Mesoscale Process, 1–4 August 2011, Los Angeles, CA*. American Meteorological Society: Boston, MA. http://www.hko.gov.hk/publica/reprint/r975.pdf

